Nanocomposites-based targeted oral drug delivery systems with infliximab in a murine colitis model

JungMin Kim

Department of Medicine
The Graduate School, Yonsei University

Nanocomposites-based targeted oral drug delivery systems with infliximab in a murine colitis model

Directed by Professor Jae Hee Cheon

The Doctoral Dissertation submitted to the Department of Medicine the Graduate School of Yonsei University in partial fulfilment of the requirements for the degree of Doctor of Philosophy

JungMin Kim

June 2020

This certifies that the Doctoral

Dissertation of JungMin Kim is approved.

Thesis Supervisor: Jae Hee Cheon

Thesis Committee Member #1: Min Goo Lee

Thesis Committee Member #2: Tae Il Kim

Thesis Committee Member #3: Soo Jeong Lim

Thesis Committee Member #4 Hyun Jung Lee

The Graduate School

Yonsei University

June 2020

ACKNOWLEDGEMENTS

I would like to thank my supervisors, Professors Jae Hee Cheon, Min Goo Lee, Tae Il Kim, Soo Jeong Lim, and Hyun Jung Lee, and my colleagues for their generous help. I would like to express my sincere gratitude to Professor Cheon or for all his assistance in overseeing this project. I thank Professor Kim for his advice on writing this thesis from the protocol for thesis. I thank Professor Lee and Professor Lim, who gave me direction and taught me the important elements of this thesis, and Professor Lee, who gave her advice and thoughts during my research and thesis writing process. I would also like to thank Da Hye Kim and Seung Won Kim for all their assistance in overseeing this project on daily basis. Last, I am grateful to my father, mother, and younger sister for always giving me infinite power and faith.

<TABLE OF CONTENTS>

LIST OF FIGURES

LIST OF TABLES

ABSTRACT

Nanocomposites-based targeted oral drug delivery systems with infliximab in a murine colitis model

Jung Min Kim

Department of Medicine
The Graduate School, Yonsei University

(Directed by Professor Jae Hee Cheon)

Infliximab (IFX), a tumor necrosis factor (TNF)-α blocking chimeric monoclonal antibody, induces clinical response and mucosal healing in patients with inflammatory bowel disease (IBD). However, systemic administration of this agent causes unwanted side effects. Oral delivery of antibody therapeutics might be an effective treatment strategy for IBD compared to intravenous administration. We developed a colon-specific drug delivery system for the oral administration of IFX using ternary nanocomposite carriers.

Nanocomposite carriers consisting of liposomes, aminoclay-coated liposomes (AC-L), Eudragit S100 AC-L (EAC-L), or those carrying IFX (IFX-L, AC-IFX-L, and EAC-IFX-L) were orally administered to mice with dextran sulfate sodium-induced colitis. We evaluated the effects of nanocomposite carriers on lymphocytes and monocytes in peripheral blood mononuclear cells (PBMC) of IBD patients. We studied the

therapeutic effects of the nanocomposites themselves and nanocomposites with IFX at target sites *in vivo* and *in vitro*.

All three carriers had a high encapsulation efficiency, narrow size distribution, and minimal systemic exposure. There was a higher interaction between nanocomposite carriers and monocytes, compared to lymphocytes in the PBMC of IBD patients. Orally administered nanocomposite carriers targeted to inflamed colitis reduced systemic exposure. All IFX delivery formulations with nanocomposite carriers had a significantly less colitis-induced body weight loss, colon shortening and histomorphological score, compared to the DSS-treated group. AC-IFX-L and EAC-IFX-L showed significantly higher improvement of the disease activity index, compared to the DSS-treated group. In addition, AC-IFX-L and EAC-IFX-L alleviated pro-inflammatory cytokine expressions (Tnfa, Il1b, and Il17). We present orally administered antibody delivery systems which improved efficacy in murine colitis while reducing systemic exposure. These oral delivery systems suggest a promising therapeutic approach for treating IBD.

Key Words: inflammatory bowel disease, infliximab, nanocomposite carrier, oral delivery system

Nanocomposites-based targeted oral drug delivery systems with infliximab in a murine colitis model

Jung Min Kim

Department of Medicine
The Graduate School, Yonsei University

(Directed by Professor Jae Hee Cheon)

I. Introduction

Inflammatory bowel disease (IBD) is a chronic relapsing inflammatory condition of the gastrointestinal tract. Cytokines are essential mediators of IBD pathophysiology and tumor necrosis factor (TNF)-α has a crucial function in the initiation and perpetuation of IBD.[1] TNF-α alters epithelial integrity, disrupts barrier function, and promotes the breakdown of intestinal homeostasis.[2] Moreover, the binding of TNF-α to the TNF receptor is associated with the prevention of apoptosis and prolongation of pro-inflammatory T cell survival in colitis.[3] Increased blood monocyte recruitment into the gut of IBD patients generates macrophages that lead to the secretion of inflammatory cytokines such as TNF, IL-6, and IL-23[4]

Therapeutic monoclonal antibodies against TNF-α are used to treat IBD.[5,6] Monoclonal antibodies have some advantages in terms of stability, bioavailability, and superior antigen targeting affinity. Infliximab (IFX) is a mouse/human chimeric monoclonal immunoglobulin G1 (IgG1) antibody against TNF-α. It directly neutralizes the biological activity of TNF-α and is more effective at inducing clinical remission of IBD and mucosal healing than conventional drugs.[7,8] However, IFX has infrequent but serious side effects such as infectious complications, autoimmune

responses, and malignancy.[9-11] Furthermore, repeated intravenous administration of IFX is costly and associated with poor compliance.[12] Ideally, an anti-TNF antibody therapy for IBD would be delivered directly to the intestinal inflammatory sites, avoiding systemic exposure, and immunosuppression.

Liposome is an attractive drug carrier; it has high biocompatibility and biodegradability, low toxicity, and non-immunogenic properties. Liposomes are mainly composed of phospholipids, and the release rate depends on the number of phospholipid bilayers.[13] Phospholipid barriers block the action of enzymes, acids, and free radicals, and protect the cargo from breaking down until it reaches the target site and is released. Specific pH range-triggered release and liposome encapsulation delay drug release specific to the gastrointestinal tract, which enhance therapeutic efficiency. Liposome-encapsulated IFX was observed to have therapeutic efficacy in autoimmune uveoretinitis.[14] In addition, liposomes provide better recovery of impaired epithelial barrier function than control in a dose-dependent manner.[15] Because ideal colon-specific delivery systems require the prevention of premature drug release, the properties of the liposome surface coating material encapsulating the anti-TNF-α agent are important because they affect the efficiency of the delivery system. Ideal colon-specific delivery systems require the prevention of premature drug release before reaching the target site. Aminoclay is a synthesized organoclay 3-aminopropyl functionalized magnesium phyllosilicate. Oral delivery systems designed with aminoclay complex enhance the bioavailability of low solubility/high permeability drugs.[16] Indeed, aminoclay is less cytotoxic and can reduce cargo dosages while enhancing delivery efficiency and allowing for the loading of macromolecules.[17] However, the therapeutic effect or effect on impaired barrier function in IBD via aminoclay-anti-TNF-α complex has not been reported.

Eudragit (methacrylic acid copolymer) is a pH sensitive coating polymer.[18] Eudragit with prednisolone was reported to efficiently degrade and deliver drugs only at colon-specific pH both *in vivo* and *in vitro*, thus minimizing drug side effects.[19] In addition, Eudragit was able to deliver 5-aminosalicylic acids (5-ASA) to the target site with

minimal systemic absorption.[20] Furthermore, the Eudragit coating system was demonstrated to have a higher mucosa-adhesive ability than control coating systems.[21] However, no studies of Eudragit encapsulating anti-TNF-α have been reported *in vivo* or *in vitro.*

Therefore, the aim of the current study was to evaluate the effectiveness and safety of new colon-targeted drug delivery systems using ternary nanocomposite carriers in a murine colitis model. Furthermore, we aimed to assess the drug delivery systems' clinical responses and therapeutic potential.

II. MATERIALS AND METHODS

1. Ethics Statement

Peripheral blood from patients with IBD was collected and analyzed after obtaining informed written consent according to the approval of the Institutional Review Board (IRB) of Severance Hospital, Yonsei University (IRB Approval No: 4-2020-0010).

Animal studies were approved by the Institutional Animal Care and Use Committee (IACUC) of Yonsei University Severance Hospital, Seoul, Korea (IACUC Approval No: 2018–0174). All methods were carried out in accordance with relevant guidelines and regulations.

2. Reagents and Materials

1,2-Dimyristoyl-sn-glycero-3-phosphocholine (DMPC) and 1,2-dimyristoyl-sn-glycero-3-phosphorylglycerol sodium salt (DMPG) were purchased from Avanti Polar Lipid Inc. (Alabaster, AL, USA). Cholesterol (Chol), α-tocopherol, bovine serum albumin (BSA) fluorescein isothiocyanate conjugate (FITC-BSA), ammonium persulfate, pepsin, pancreatin, and Remicade® (IFX) were purchased from Sigma-Aldrich (St. Louis, MO, USA). Cy™7 Mono NHS Ester was purchased from GE Healthcare (Little Chalfont, Buckinghamshire, UK). BCA Protein Assay Kit and PageRuler Prestained Protein Ladders were purchased from Thermo Fisher Scientific (Waltham, MA, USA). Sodium dodecyl sulfate (SDS) was purchased from Kracker

Scientific (NY, USA). Coomassie-brilliant blue R-250 staining solution, 30% acrylamide/Bis solution (29:1), TEMED, 4× Laemmli sample buffer, 1.5 M Tris-HCl buffer and 0.5 M Tris-HCl buffer were purchased from Bio-Rad Laboratories (Hercules, CA, USA). Magnesium chloride hexahydrate (98%) and other inorganic salts were purchased from Junsei Chemical Co. (Tokyo, Japan) Eudragit® S100 was kindly donated by Evonik Korea (Seoul, Korea).

3. Preparation of liposomes

DMPC, Chol, DMPG, and α-tocopherol were mixed at a molar ratio of 26:10:2:2 in tertiary butyl alcohol. The mixtures were frozen at -80℃ overnight followed by freeze-drying for 24 h. The obtained lipid cakes (total 40 μmol of lipid mixture) were hydrated with 1 mL of IFX solution, which was produced by dissolving Remicade powder in distilled water (10 mg/mL), or FITC-BSA solution in phosphate-buffered saline (pH 7.4). The hydrated liposome dispersions were vortexed and sonicated for 1 h at 24℃ of DMPC by using an ultrasonic cleaning bath. To obtain a liposomal dispersion with increased homogeneity and reduced particle size, additional sonication was carried out by using a cell disruptor as previously described.[22] Liposome dispersions were then subjected to freeze-thawing for five cycles of 5 min incubation at -180℃ and 15 min incubation at 37℃ to improve protein encapsulation. To remove non-encapsulated proteins, liposomes were collected by centrifugation at 43,000 × g for 1 h at 4℃. The resulting pellets were re-suspended in the original volume of phosphate-buffered saline (PBS). The prepared liposomes were stored at 4℃ until use.

4. Coating of liposomes

The 3-aminopropyl-functionalized magnesium phyllosilicate (aminoclay) was synthesized by following a method described previously.[23] Before coating, the bulk aminoclay powder was dispersed in water, followed by ultrasonication for 10 min for the exfoliation of the aminoclay. Aminoclay-coated liposomes (AC-L) were obtained

by spontaneous assembly of positively charged aminoclay on negatively charged liposomal surfaces. Briefly, equal volumes of liposome dispersions (pre-diluted with distilled water to give a lipid concentration of 10 mg/mL) were added dropwise to exfoliated aminoclay dispersion (10 mg/mL) to give a lipid/clay weight ratio of 1:1. The mixture was incubated at 25℃ for 30 min with stirring and then centrifuged at 15,000 × g for 7 min at 4℃. The resulting aminoclay-liposome pellets were re-suspended in 1 mL of PBS.

For further coating of clay-liposomes with Eudragit S-100, an equal volume of clay-liposome dispersions pre-diluted to a concentration of 2.5 mg lipid per mL and was added dropwise to 0.1% Eudragit S100 solution in PBS. The mixture was incubated at 4℃ for 30 min with stirring and then centrifuged at 15,000 × g for 7 min at 4℃. The resultant Eudragit S100-coated aminoclay-liposome (EAC-L) pellets were re-dispersed in the original volume of PBS.

5. Physicochemical characterization of liposomes

The mean particle size and polydispersity index of nanocomposite carriers were measured by dynamic light scattering using a fiber-optics particle analyzer as described in our earlier study.[15] Particle size analysis data were assessed using the CONTIN program provided by the manufacturer. Zeta potential (the electrical potential at the shear plane of the nanoparticle) was measured using a Zetasizer Nano ZSP (Malvern, UK). Samples were diluted 50-fold with de-ionized water before measuring to reach the analytical measurement range that was automatically set. Default instrument settings and automatic analysis were used for all measurements. We performed each measurement in duplicate and selected the average of the measurements.

The diameter and morphology of liposomes were imaged by negative-stain transmission electron microscopy. Liposome samples were 50-fold diluted with PBS solution and dropped on a 200-mesh copper grid coated with carbon, and negatively stained with 2% uranyl acetate for 1 min. Excess stain was removed and the samples

were allowed to air-dry completely. Dried samples were examined using a Tecnai G2 Spirit (FEI company, Hillsboro, OR, USA) operating at 120 keV.

The encapsulated concentration of IFX and FITC-BSA were determined by BCA protein assay or by measuring the fluorescence of FITC (excitation 490 nm, emission 525 nm) with a fluorescence spectrometer after disrupting the liposome dispersions with an equal volume of 10% SDS (fluorescence assay) or ethanol (BCA assay). Standard curves, pre-constructed with serial dilutions of FITC-BSA with ethanol, were used to convert fluorescence to FITC-BSA concentration. The stability of BSA in the nanocomposite carriers was investigated using circular dichroism spectroscopy.

6. Gastrointestinal stability of liposomes

To evaluate the physical stability of liposomes in the gastrointestinal tract, time-dependent protein release from BSA-entrapped liposomes in simulated gastrointestinal conditions was assessed using dialysis. Briefly, 900 μL of each liposome dispersion (BSA-L, AC-BSA-L, and EAC-BSA-L) and free FITC-BSA solution pre-adjusted to 250 μg of BSA per mL were separately placed in a Float-A-Lyzer (MWCO 1,000 kDa) and dialyzed with 30 mL PBS, simulated gastric fluid (SGF; 2 g NaCl/1 L water, pH 1.2) or simulated intestinal fluid (SIF; 6.8 g KH2PO4/1 L water, pH 6.8), respectively, at 37℃. At predetermined time points (1 min, 1, 2, 4, 6, 8, and 24 h), aliquots of each sample were taken from the media and the amount of FITC-BSA released from liposomes was quantified by measuring the fluorescence as described above. The gastrointestinal stability of liposomes was evaluated by monitoring changes in the size of liposomes (50 μL) incubated with 950 μL of PBS, SIF, or SGF at 37℃.

7. Protein stability analysis

To assess the gastrointestinal stability of the protein encapsulated in liposomes after incubation of BSA encapsulated liposomes with SIF or SGF, gel electrophoresis was performed. FITC-BSA (400 μg/mL), as a free solution or encapsulated in liposomes

(liposome, Aminoclay coated liposome, and Eudragit S100-aminoclay coated liposome), was incubated with an equal volume of PBS, SGF (with or without supplementation with 3.2 g/L pepsin), and SIF (with or without supplementation with 10 g/L pancreatin) at 37℃ for a designated time. Aliquots taken from each sample were mixed with 4× sample buffer, and then 20 μL of the mixture was loaded on an 8% SDS-polyacrylamide gel. Electrophoresis of samples was performed at a constant voltage of 120 volts using a PowerPac BasicTM (Bio-Rad, CA, USA) in SDS-PAGE buffer (25 mM Tris, 18.8 g glycine, 1 g SDS, and 1 L distilled water). After electrophoresis, the gels were stained with Coomassie-brilliant blue R-250 solution for 1 h and then destained in destaining buffer (aqueous solution of 40% methanol and 10% acetic acid). The percentage of intact parent protein (FITC-BSA) at different time intervals was calculated as follows:

Intact BSA% = Dt/DT × 100,

where Dt is the intensity of the intact FITC-BSA at time interval t, and DT is the intensity of the intact FITC-BSA before digestion.

8. Experimental animals

Twenty-two to twenty three male eight-week-old C57BL/6 mice were kept under standard conditions at a temperature of 21-22℃, under a 12 h light/dark cycle and allowed to acclimate for a week before starting the experiment. Body weight and physical activity were monitored daily.

9. Distribution of nanocomposite carriers in dextran sulfate sodium (DSS) colitis mice

To assess the biodistribution of nanocomposite carriers after oral administration, Cyanine-7 (Cy7)-labeled nanocomposite carriers were prepared. Briefly, two μg of Cy7 was dissolved with 40 μmol of DMPC:Chol:DMPG:α-tocopherol (26:10:2:2) mixture in tertiary butyl alcohol. The liposomes were prepared from the mixture as described above, except that the unentrapped Cy7 was separated from the liposomes

by dialysis. Each liposome dispersion was adjusted to 0.44 μg/mL before oral administration.

Colitis was induced in mice by oral administration of 1.5% (wt/vol) DSS (36-50 KD molecular weight, MP Biomedicals, Solon, OH, USA) for 5 days in drinking water. After fasting for 12 h, Cy7.0-L, Cy7-AC-L, and Cy7-EAC-L were orally administered to mice with DSS-induced colitis at a dose of 20 mg/kg in a volume of 100 μL PBS. Control mice maintained normal drinking water for 5 days and then Cy7.0-EAC-L was administered orally at a dose of 20mg/kg in a volume of 100 μL PBS. Mice were sacrificed 7 h after administration of Cy7.0-labeled nanocomposite carriers. Cy7.0-labeled nanocomposite carriers were visualized (Cy7: excitation 750 nm, emission 773 nm) and analyzed by using an in vivo image analyzer (Caliper IVIS Lumina II, Caliper Life Science, USA).

10. DSS-induced colitis and therapeutic effect of nanocomposite carriers

To test the therapeutic effect of nanocomposite carriers, colitis was induced in mice by administering 1.5% DSS in their drinking water for 7 days. Mice were randomly divided into five groups: DSS only (DSS-treated control group), DSS-treated with L (L group), DSS-treated with AC-L (AC-L group), DSS-treated with EAC-L (FAC-L group), DSS-treated with intra-peritoneal IFX (IP-IFX group), and DSS-treated with per-oral IFX (PO-IFX group. Mice in the L, AC-L, and EAC-L groups were orally administered nanocomposite carriers (10mg/kg) once daily, for 9 days, from day 0. The dose of nanocomposite carriers (10 mg/kg for all groups) was predetermined to have an optimal therapeutic effect. Mice received 4 mg/kg of IFX in 200 μL PBS daily by oral or intraperitoneal administration for nine consecutive days. The dose of IFX was determined to have an optimal therapeutic effect based on existing studies.[24,25] Drinking water was replaced with pure water and maintained for 2 days. Changes in body weight, stool consistency, and presence of blood in the stool or at the anus were measured daily throughout the study period. Mice were sacrificed at day 12; spleen and colons were collected to assess the therapeutic efficacy of the

nanocomposite carriers. Disease activity index (DAI) was evaluated using the summed score of three factors (weight loss, stool consistency, and bleeding).[26]

11. DSS-induced colitis and therapeutic effect of nanocomposite carriers-IFX conjugates (IFX-L, AC-IFX-L, EAC-IFX-L)

To test the therapeutic effect of nanocomposite carriers loaded with IFX, colitis was induced in mice via the addition of 1.5% DSS to drinking water for 7 days. Drinking water was then replaced with pure water for 4 days. Mice were sacrificed on day 11. Mice were orally administered 200 μL PBS, IFX-L (10 mg/kg), AC-IFX-L (10 mg/kg), EAC-IFX-L (10 mg/kg), or PO-IFX (10 mg/kg) once daily, from day 0 to day 8 (total 9 days). The dose of nanocomposite carriers and IFX was predetermined to have an optimal therapeutic effect.[24,25] Flow cytometry, qRT-PCR, analysis of TNF-α by enzyme-linked immunosorbent assay (ELISA), and western blotting are described in the Supplementary Information section.

12. Histology

Colon tissues were fixed in 10% neutral formalin and then embedded in paraffin. Tissues were stained by hematoxylin and eosin and periodic acid Schiff (PAS) staining. The severity of colitis was scored as described previously.[27] Goblet cell staining was scored from 0 to 3 (3, minimal, <20%; 2, mild, 21–35%; 1, moderate, 36–50%; 0, marked, >50%).

13. Goblet cell counting

Colonic tissue sections were processed with PAS staining. Stained goblet cells were counted per crypt. Maximum 52 and minimum 20 fully conserved crypts on each section were examined, and the average numbers were marked as a representative goblet cell count of each section.

14. Flow cytometry

Whole blood from four patients with ulcerative colitis (UC) and five with Crohn's disease (CD) was collected in EDTA tubes and processed shortly after collection. Whole blood in EDTA (10 mL), was diluted with 10 mL of Dulbecco's PBS and loaded into Leucosep tubes (Greiner Bio-One, Frickenhausen, Germany). Human peripheral blood mononuclear cells (PBMC) were purified by Ficoll-Paque density gradient centrifugation (GE Healthcare Bio-Sciences AB, Sweden). Cells were separated at 1,500 × g for 15 min at 4℃, according to the manufacturer's instruction. The supernatant was transferred to a new tube, centrifuged at 200 × g for 5 min at room temperature, then gently poured off and discarded. The remaining red blood cells were incubated in 10 mL of lysis buffer for 30 min at room temperature in the dark. Cells were separated at 200 × g for 5 min at room temperature, then supernatant was carefully removed. The PBMCs were washed in Dulbecco's PBS and centrifuged at 200 × g for 5 min at room temperature. Five milliliters of culture medium (RPMI 1640 containing 1% penicillin/streptomycin and 10% FBS) were diluted to 1/10 and PBMCs underwent MACS® bead isolation. PBMC cultures (1×10^5 - 1×10^6 cell/mL) were treated with four types of drug delivery carriers (free BSA, BSA-L, AC-BSA-L, and EAC-BSA-L) 8 ㎍/mL (1×10^5 cells) and incubated at 37℃ for 4 h. Cell suspensions were stained on ice for 30 min in the dark with various combinations of directly fluorochrome-conjugated antibodies; CD3 (V500), CD4 (PerCP/Cy 5.5), or CD11b (APC), in permeabilization buffer (BD). Flow cytometry analysis was performed using a FACSVerse flow cytometer (BD Biosciences, San Jose, CA) and analyzed using FlowJo software (Tree Star, San Carlos, CA, USA). Patient characteristics are described in Table 1 and human antibodies to cd3, cd4, and cd11b are described in Table 2.

Table 1. Patient characteristics

	CD	UC
n (male/female)	5 (3/2)	4 (2/2)
Age[a]	25.0 ± 1.5	41.3 ± 6.5

Disease duration of UC / CD[a]	5.3 ± 2.4	1.5 ± 1.3
UCAI/CDAI[a]	178.0 ± 72.5	3.8 ± 1.4
ESR, mm/hr[a]	19.6 ± 12.5	8.3 ± 2.4
CRP, mg/L[a]	4.1 ± 2.2	0.8 ± 0.2
Disease location[b]		
Ileum	0	
Colon	0	
Ileocolonic	5 (100)	
Cecum		1 (25)
sigmoid colon		2 (50)
Rectum		1 (25)
Prior intestinal resections	0	0
Medication[b]		
Sulphasalazine/5-ASA	2 (40)	4 (100)
Immunosuppressive treatment	1 (20)	0
Corticosteroids	0	2 (50)
Anti-TNFα	1 (20)	0
Anti-IL-12/IL-23	1 (20)	0

5-ASA: 5-aminosalicylates; CD: Crohn's disease; CDAI: Crohn's Disease Activity Index; CRP, c-reactive protein; ESR: erythrocyte sedimentation rate; UC: ulcerative colitis; TNF: tumor necrosis factor.
[a]Year: median ± SD; [b]*N* (%)

Table 2. Human Antibiotics Fluorescence-activated cell sorting

Antibiotics	Information
CD3	BD bioscience Clone number : UCHT1
CD4	ebioscience Clone number : OKT4 (OKT-4)
CD11b	ebioscience Clone number : ICRF44

15. Quantitative reverse-transcription polymerase chain reaction (qRT-PCR)

Total RNA was extracted using TRIzol Reagent (Life Technologies, Carlsbad, CA, USA) following the manufacturer's instructions. RNA was reverse transcribed using a High Capacity cDNA Reverse-Transcription Kit (Applied Biosystems, Warrington,

UK) according to the manufacturer's protocol. qPCR was performed using SYBR Green Master Mix in a StepOne Plus real-time PCR system. The thermal cycles were 40–45 cycles of 95℃ for 30 s, 60–63℃ for 30 s, and 72℃ for 40 s. All PCRs were run in triplicate. Relative expression was determined by the 2–ΔΔCt method. Results were reported as fold changes, compared to the control by normalizing transcription levels to β-actin. Tnfa and inducible nitric oxide synthetase (iNos) primers were purchased from Bioneer (AccuTarget, Daejeon, Korea). Other PCR primers are listed in Table 3.

Table 3. Primer sequences for quantitative real time polymerase chain reaction

Gene	Sequence (5′—3′)
Tnfα	F: CAAAGGGAGAGTGGTCAGGT R: ATTGCACCTCAGGGAAGAGT
Il1b	F: GCA ACT GTT CCT GAA CTC AAC T R: ATC TTT TGG GGT CCG TCA ACT
Il6	F: TTG CCT TCT TGG GAC TGA TG R: CCA CGA TTT CCC AGA GAA CA
Il17	F: CAG CAG CGA TCA TCC CTC AAA G R: CAG GAC CAG GAT CTC TTG CTG
Inos	F: GGC AGC CTG TGA GAC CTT TG R: GCA TTG GAA GTG AAG CGT TTC
β-Actin	F: CATCTTCACCGTTCCAGT R: GTCCACCTTCCAGCAGAT

F: forward primer, R: reverse primer

16. TNF-α detection

TNF-α was measured using a Quantikine® ELISA mouse Kit (Cat. number: MTA00B, R&D Systems, Inc., MN, USA) following the manufacturer's instruction.

17. Western blotting

Proteins were extracted from colon tissue using Pierce RIPA buffer mixed with Halt Protease & Phosphatase Inhibitor Cocktail. Quantified samples were prepared using a bicinchoninic acid protein assay kit and sample buffer with β-mercaptoethanol.

Prepared samples were boiled at 95℃ for 5 min and centrifuged at 13,000 g/min for 15 min at 4℃. The protein samples (20 μg) were loaded onto a polyacrylamide gel divided into stacking (5%) and running (10%) portions. Electrophoresis was performed in Tris-glycine SDS buffer (iNtRON Biotechnology, Sungnam, Gyeonggi, Korea). Differentiated proteins were transferred to polyvinylidene difluoride membranes for 90 min at 100-150 volts (Bio-Rad) and blocked with Tris-buffered saline with Tween-20 supplemented with 5% filtered-BSA. Primary antibodies (TNF-α, 1:2,000, Santa Cruz, CA, USA; IL-1β, 1:2,000, Santa Cruz; β-actin, 1:1,000, Santa Cruz) were diluted in 5% filtered-BSA and incubated with rocking overnight at 4℃. Membranes were washed and incubated with horseradish peroxidase (HRP)-conjugated secondary antibodies (TNF-α, goat anti-mouse IgG-HRP, 1:1,000; IL-1β, goat anti-rabbit IgG-HRP, 1:1,000) diluted in 5% filtered-BSA for 3 h. Anti-β-actin (Santa Cruz) was used as the loading control. Mouse antibodies are listed in Table 4.

Table 4. Mouse Antibiotics Western blot

Abs	Information
TNFα	TNFα (52B83): sc-52746 (Santa Cruz)
	Secondary: goat-anti-mouse-IgG-HRP (Santa Cruz)
Il1b	Il1b (H-153): sc-7884 (Santa Cruz)
	Secondary: goat-anti-rabbit-IgG-HRP (Santa Cruz)
β-actin	b-actin(C4): sc-4778 (Santa Cruz)
	Secondary: goat-anti-mouse-IgG-HRP (Santa Cruz)

18. Statistical analysis

The data were reported as mean and standard deviation. Groups were compared by performing student's *t*-test or one-way analysis of variance using Graphpad Prism software (Ver. 7.0, Graphpad, CA, USA). Results with p value < 0.05 were reported as statistically significant.

III. RESULTS

1. Characterization of nanocomposite carriers

Transmission electron microscopy images showed that BSA-FITC coated with BSA-L, AC-BSA-L, and EAC-BSA-L were spherical and surrounded the inner aqueous core containing BSA-FITC (Figure 1A). Particle size and zeta potential analysis using dynamic light scattering showed a gradual increase in particle sizes (360, 396, and 406 nm in BSA-L, AC-BSA-L, and EAC-BSA-L, respectively) and reversal of zeta potential values (-79.9, +12.6, and -55.4 mV in BSA-L, AC-BSA-L, and EAC-BSA-L, respectively) in the layer-by-layer coating. The net negative surface charge of BSA-L appeared to promote the alternating deposition of positively charged aminoclays through electrostatic interaction. The positively charged surface of AC-BSA -L allowed the deposition of anionic Eudragit S100, resulting in layer-by-layer coated EAC-BSA-L. Entrapped BSA-FITC concentrations of nanocomposites were 769 ± 14 μg/mL (BSA-L), 498 ± 85 μg/mL (AC-BSA-L) and 338 ± 15 μg/mL (EAC-BSA-L). A gradual decrease in entrapped protein concentration by coating was caused by the leakage of entrapped proteins during the layering process.

Nano-sized IFX-entrapped liposomes gradually increased in size (244, 222, and 426 nm in IFX-L, AC-IFX-L, and EAC-IFX-L, respectively) and zeta potential values were reversed (-54.8, +2.6, and -31.5 mV in IFX-L, AC-IFX-L, and EAC-BSA-L, respectively) (Figure 1B). Similar to the decrease in the concentration of nanocomposites with BSA, the entrapped concentrations of nanocomposites also decreased (2,888 ± 236, 1,480 ± 71, and 686 ± 63 μg/mL in IFX-L, AC-IFX-L, and EAC-IFX-L, respectively). Compared with BSA, IFX had a higher loading concentration, which may be due to the difference between hydrophilic and hydrophobic aa domains. IFX contains more hydrophobic parts that are more compatible with phospholipid membranes than BSA, resulting in their entrapment at higher concentrations. Collectively, these observed structural properties confirmed the successful formation of the antibody drug delivery nanocomposites of liposomes, aminoclay, and Eudragit S100.

A **B**

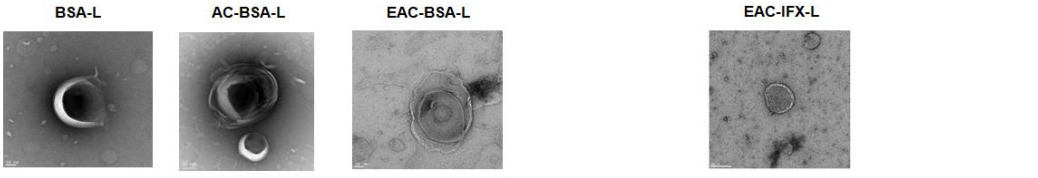

	FITC-BSA		
	liposome	AC-L	EAC-L
size (nm)	360 ± 19	396 ± 37	406 ± 23
zeta potential (mV)	-79.9 ± 0.6	+12.6 ± 0.5	-55.4 ± 0.2
Entrapped concentration (μg/mL)	769 ± 14	498 ± 85	338 ± 15

	Infliximab		
	liposome	AC-L	EAC-L
size (nm)	244 ± 22	222 ± 14	426 ± 16
Zeta potential (mV)	-54.8 ± 1.0	+2.6 ± 0.2	-31.5 ± 1.2
Entrapped concentration (μg/mL)	2888 ± 236	1480 ± 71	686 ± 63

Figure 1. C**haracteristics of nanoparticles**

(A) Transmission electron microscopy (TEM) images of fluorescein isothiocyanate (FITC)-bovine serum albumin (BSA) with nanocomposite carriers (liposome, aminoclay-coated, and Eudragit S100-clay-coated). Scale bar represents 50 μm. Liposomes were prepared with 40 μmole of DMPC:CHOL:DMPG:α-Tocopherol (26:10:2:2 molar ratio) and 10 mg of BSA-FITC per 1 mL. The zeta potential is the mean ± SD of two independent experiments (n = 2), and the size and captured concentration data are the mean ± SD of three independent experiments (n = 2) (B) TEM images of Eudragit S100-aminoclay-coated liposomes entrapped with infliximab (IFX). Scale bar represents 100 μm. Liposomes were prepared with 40 μmole of DMPC:CHOL:DMPG:α-Tocopherol (26:10:2:2 molar ratio) and 10 mg IFX per 1 mL. Size, zeta potential, and concentration of IFX encapsulated by nanocomposites were measured. AC-BSA-L, aminoclay-liposome-coated BSA; BSA, bovine serum albumin; BSA-L, liposome-coated BSA; EAC-IFX-L, Eudragit S100-liposome-coated IFX; Eudragit S100-aminoclay-liposome-coated IFX

2. Protein stability of free BSA incubated in simulated gastric fluid and simulated intestinal fluid

We assessed the physical stability of BSA-entrapping nanocomposite carriers under simulated gastrointestinal conditions by using the dialysis method. The protein integrity profile of free BSA before and after exposure to SGF or SIF is shown in

Figure 2. When free BSA solution was incubated in SGF without pepsin supplementation, no significant change in the BSA-corresponding protein band was observed, indicating the high protein stability of BSA under the experimental conditions (Figure 2A). The complete loss of the BSA band was observed after 1-min incubation in SGF supplemented with pepsin, indicating a rapid protein degradation induced by enzymatic action (Figure 2B). In SIF supplemented with pancreatin, protein degradation was slower than control but occurred in a time-dependent manner (Figure 2C). The decrease in the protein band of BSA obtained from incubation of nanocomposite carriers (BSA-L, AC-BSA-L, and EAC-BSA-L) was much less and slower in both SGF and SIF (supplemented with pepsin or pancreatin) (Figure 2D, E), compared to free BSA solution.

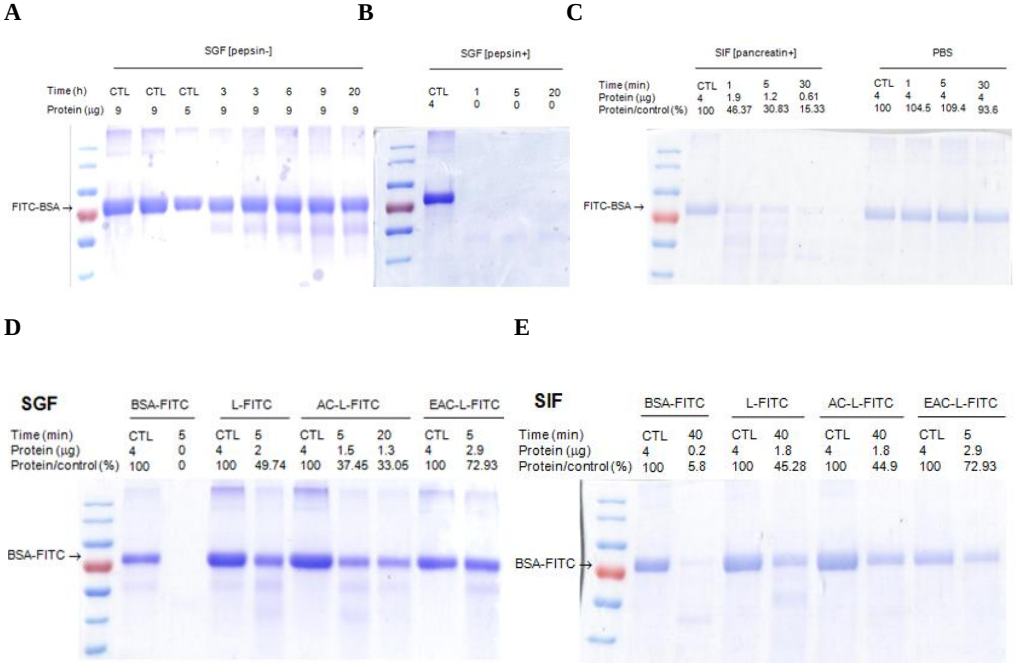

Figure 2. **Protein stability of BSA entrapped by nanocomposites**.

Protein stability of free bovine serum albumin (BSA) incubated in (A) SGF without pepsin, (B) SGF with pepsin, and (C) SIF with pancreatin, compared to the PBS at 37^{o}C for indicated time periods. For (B) and (C), samples corresponding to 4 μg

FITC-BSA were subjected to gel electrophoreses. The molecular weight of FITC-BSA was 70 KDa. SDS-PAGE gel stained by Coomassie blue R-250. Protein stability of BSA incubated in (D) SGF with pepsin and (E) SIF with pancreatin as a free form or as a form encapsulated in liposomes (uncoated, Aminoclay-coated or Eudragit® S100-aminoclay-coated liposomes). Samples corresponding to 4 μg FITC-BSA were subjected to gel electrophoreses.

3. BSA release profile from liposomes incubated in phosphate-buffered saline, simulated gastric fluid, or simulated intestinal fluid

Particle size changes and protein release profiles from the three nanocomposite carriers were also examined in PBS, SGF, or SIF (Figure 3). Eudragit S-100 is a pH sensitive formulation that decomposes above pH 7,[28] and because Eudragit coating does not peel off from PBS and SIF, the size of nanocomposite carriers was unchanged (Figure 3A). All of the tested nano-formulations were observed to have delayed and reduced drug release (Figure 3B). In particular, EAC-BSA-L showed minimal drug release in SIF for 2 h, suggesting its superior ability to retard premature protein drug release. In SGF, only EAC-BSA-L increased in size as soon as it was added to SGF. However, because there was no change in size until 8 h and there was no change of protein structure in circular dichroism data, EAC-BSA-L existed as a weak aggregate between particles under acidic conditions, but there was no change in the structure of nanocomposite carriers.

In PBS incubation, the spectra of free BSA and the other three nanocomposite encapsulated BSAs (BSA-L, AC-BSA-L, and EAC-BSA-L) were different (Figure 3C). This may be due to the separation of the liposomes, caused by adding SDS just before the circular dichroism measurement, to isolate the BSA inside the liposome. Collectively, the α-helix structure of BSA with nanocomposite carriers was much better maintained than free BSA groups, whereas the those structure of free BSA was broken under SGF (pepsin +) conditions for 1 h. In addition, BSA encapsulated in EAC--BSAL remained nearly intact. These results indicated the successful fabrication

of drug delivery nanocomposite carriers with the ability to safely and slowly release encapsulated cargo under gastric and intestinal conditions.

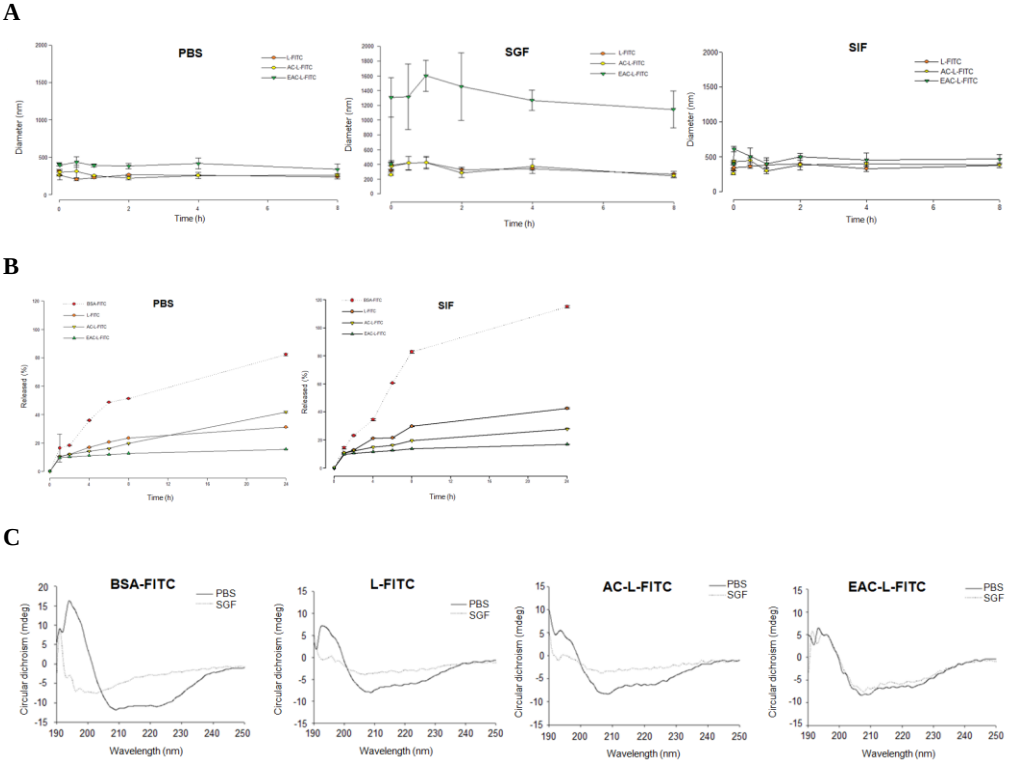

Figure 3. In vitro drug release of nanocomposite carriers

(A) Time-dependent fluorescein isothiocyanate-bovine serum albumin (FITC-BSA) release profile from liposomes incubated in phosphate-buffered saline (PBS) or semulated intestinal fluid (SIF, without pancreatin), at 37°C. (B) Time-dependent fluorescein isothiocyanate-bovine serum albumin (FITC-BSA) release profile from liposomes incubated in phosphate-buffered saline (PBS) or simulated intestinal fluid (SIF, without pancreatin) at 37℃. (C) Circular dichroism analysis of the BSA stability in the nanocomposites.

4. Targeting ability of nanocomposite carriers

To confirm targeting ability, we performed an *in vivo* drug targeting study using Cy7-

labeled nanocomposite carriers in mice with DSS-induced colitis fed a purified diet AIN-76A (Table 5). At 7 h post-administration of the Cy7 labeled delivery carriers, fluorescence imaging showed stronger Cy7 fluorescence signal in the colon and a significant but weaker Cy7 fluorescence signal in the small intestine (Figure 4A, B). In the cecum and colon without colitis, EAC-L group exhibits higher fluorescence signals. In contrast, other organs (heart, lung, liver, spleen, pancreas, and kidney) did not show significant Cy7 fluorescence signals (Figure 4C). The average radiant efficiency of all nanocomposite carriers in the inflamed colon was increased. The AC-L treated mice with the inflamed colon had higher values than DSS only group and mice treated with EAC-L without colitis had higher values than control groups (Figure 4D). These results of the bio-distribution study using Cy7 indicate no significant systemic exposure of nanocomposite carriers orally administered to target inflamed colon.

Table 5. Mouse diet *in vivo* imaging system

Abs	Information
AIN-76A	ENVIGO
Purified Diet	Cat NO: 170481

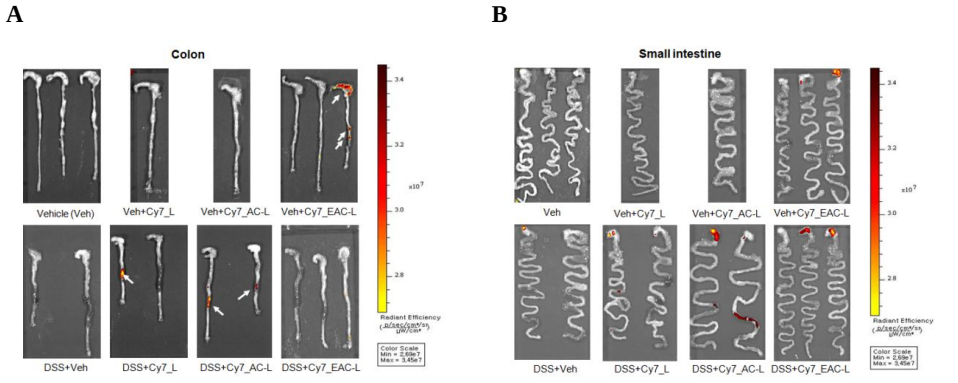

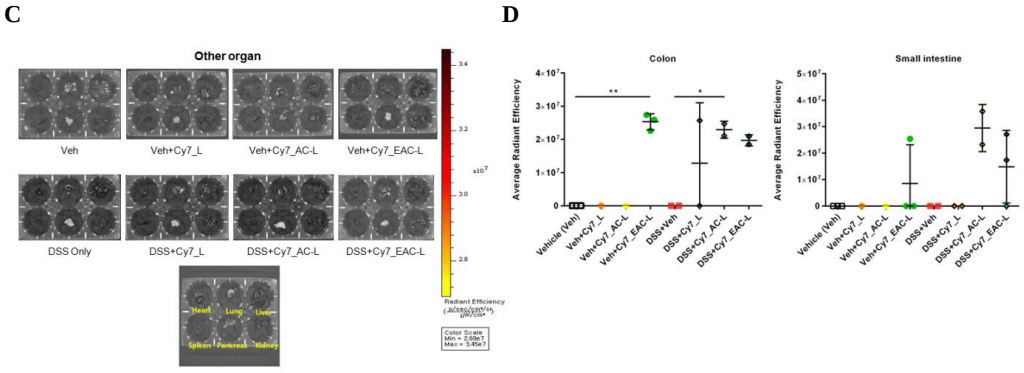

Figure 4. Ex-vivo fluorescence images of the gastrointestinal tract of mice after oral administration of Cyanine7-labeled liposomal formulations

Images were obtained 7 h after oral administration of Cy7-labeled delivery carriers using an in vivo imaging system (IVIS). (A) Fluorescence of Cy7 measured in the inflamed colon was observed in all drug delivery carrier groups. Arrows indicate strong fluorescence signals at the site of inflammation (B) In inflamed small intestine, the AC-L group and EAC-L group were measured for fluorescence of Cy7 (C) fluorescence images of Cy7 in a multi-well format obtained from organs (heart, lung, liver, spleen, pancreas, and kidney). (D) average radiant efficiency of drug delivery formulations distributed in inflamed intestine in comparison to normal conditions. Data representative of six independent groups with n = 3 mice/group (Vehicle group), n = 1 mice/group (Vehicle with Cy7 labeled L), n = 1 mice/group (Vehicle with Cy7 labeled AC-L), n = 3 mice/group (Vehicle with Cy7 labeled AC-L), n = 2 mice/group (DSS colitis with vehicle), n = 2 mice/group (DSS colitis with Cy7 labeled L), n = 2 mice/group (DSS coltis with Cy7 labeled AC-L), n = 2 mice/group (DSS colitis with Cy7 labeled EAC-L). Data are expressed as means ± SD. *, $p < 0.05$; **, $p < 0.01$; ***, $p < 0.001$; ****, $p < 0.0001$. Statistical significance was assessed using Student's t-test (d) and one-way ANOVA followed by Dunnett post-test. Control, treated with vehicle; DSS+Cy7_AC-L, DSS colitis with aminoclay-liposome-coated Cy7; DSS+Cy7_EAC-L, DSS colitis with Eudragit S100-liposome-coated Cy7; DSS+Cy7_L, DSS colitis with liposome-coated Cy7.

5. Nanocomposite carriers enhance the anti-inflammatory capacity of intestinal macrophages

The potent anti-inflammatory capacity of both T cells and monocytes have a crucial function in colitis. Dysregulation of CD4 T helper (Th) cells and their signature cytokines can contribute to IBD pathogenesis.[29] TNF-α secretion was significantly increased by inflamed lamina propria monocytes in IBD patients. In addition, the clinical severity of IBD (UC, and CD) and serum TNF-α level are correlated.[30,31] To evaluate the effects of nanocomposite carriers (L-FITC, AC-L-FITC, and EAC-L-FITC) on lymphocytes ($CD3^+CD4^+$ cells) and monocytes ($CD11b^+$ cells) in PBMCs of IBD patients, we observed a subset of $CD3^+CD4^+$ T cells and $CD11b^+$ monocytes (Figure 5A). The mean fluorescence intensity (MFI) values of nanocomposite carriers in lymphocytes are between 1,000 and 3,000, and those of nanocomposite carriers in monocytes are between 3,000 and 15,000. Lymphocytes of UC patients had significantly higher MFI values in the all nanocomposite carrier groups compared to the BSA-FITC group, whereas monocytes in UC patients did not differ significantly from those of BSA-FITC group (Figure 5B). The EAC-L-FITC group had significantly higher MFI values in the lymphocytes and monocytes of CD patients compared to the BSA-FITC group. AC-L-FITC group had significantly a higher MFI value in lymphocytes of CD patients than BSA-FITC group, but there was no difference in monocytes. These results suggest that nanocomposite carriers may have a higher absorption into monocytes than lymphocytes, and that absorption into lymphocytes show a significant difference between carriers.

A

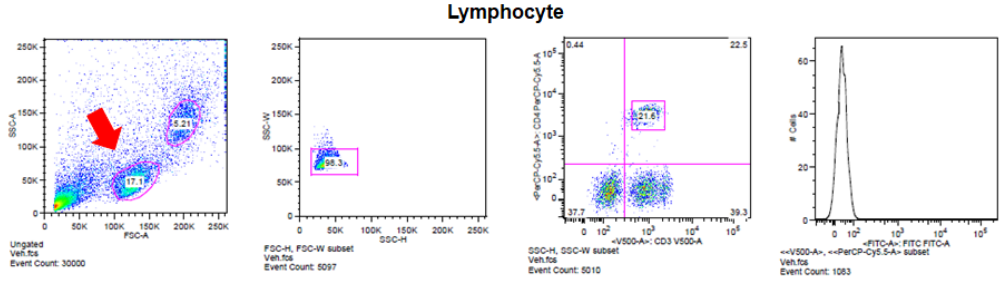

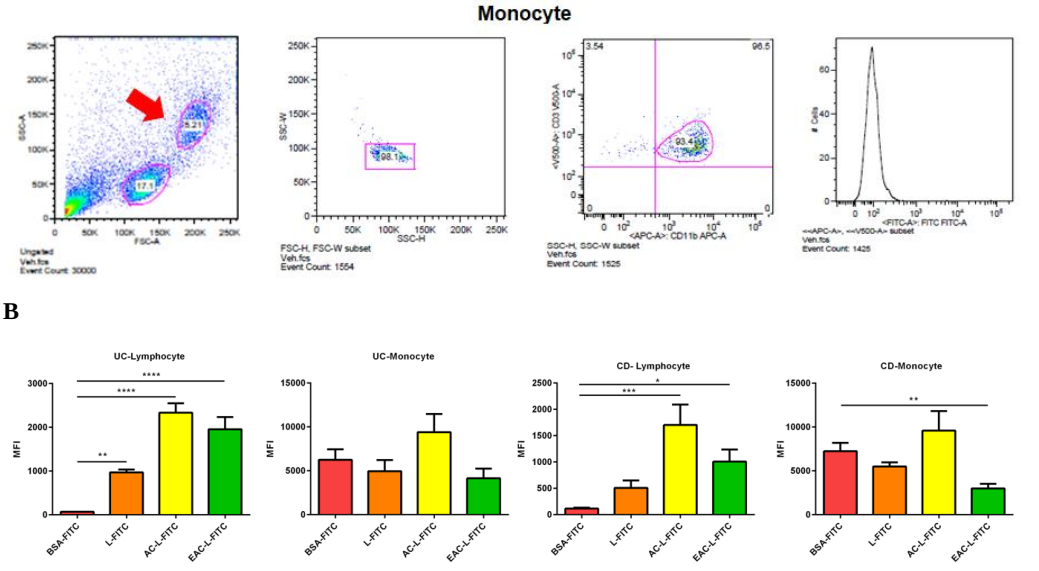

Figure 5. Drug delivery formulations in vitro

(A) Representative flow cytometry dot plot. Diagrams of flow cytometry gating the lymphocytes and monocytes of UC and CD patients. CD subset of T lymphocyte (CD3 and CD4) and macrophage (CD11b) in produced by peripheral blood mononuclear cells (PBMC) of IBD patients (B) median fluorescence intensities (MFIs) of BSA-FITC with drug delivery formulations between UC and CD patients. Data are expressed as means ± SD. *, $p < 0.05$; **, $p < 0.01$; ***, $p < 0.001$; ****, $p < 0.0001$. Statistical significance was assessed using Student's t-test (D) and one-way ANOVA followed by Dunnett post-test. AC-L-FITC, aminoclay-liposome-coated FITC; BSA-FITC, bovine serum albumin-coated FITC; L-FITC, liposome-coated FITC; EAC-L-FITC, Eudragit S100-liposome-coated FITC

6. Liposome itself alleviates inflammation in DSS colitis mice

We examined the therapeutic effects of L, AC-L, EAC-L, IFX via oral administration, and IFX via intraperitoneal injection (10 mg/kg, 200 μL) in mice with DSS-induced colitis (Figure 6A). Our results showed that liposome-treated mice had a significantly less colitis-induced body weight loss and colon shortening (Figure 6B, C). In addition,

mice treated via intraperitoneal injection of IFX had a significant reduction of colon shortening (Figure 6C). These results were further supported by DAI findings (Figure 6D). In the PAS-stained colon tissue indicated that mice treated with liposomes (L group) or IFX via intraperitoneal injection (IP-IFX group) had less colon tissue damage and inflammatory cell infiltration than those treated with other nanocomposite carriers or control group (Figure 6E). Histomorphological scores were significantly lower in mice treated with L and IP-IFX, compared to the DSS inflammation group, whereas goblet cell scores were not significantly different between all treatment groups. These results suggest that drug delivery via liposome encapsulation is superior to other nanocomposite carriers in terms of its anti-inflammatory effects.

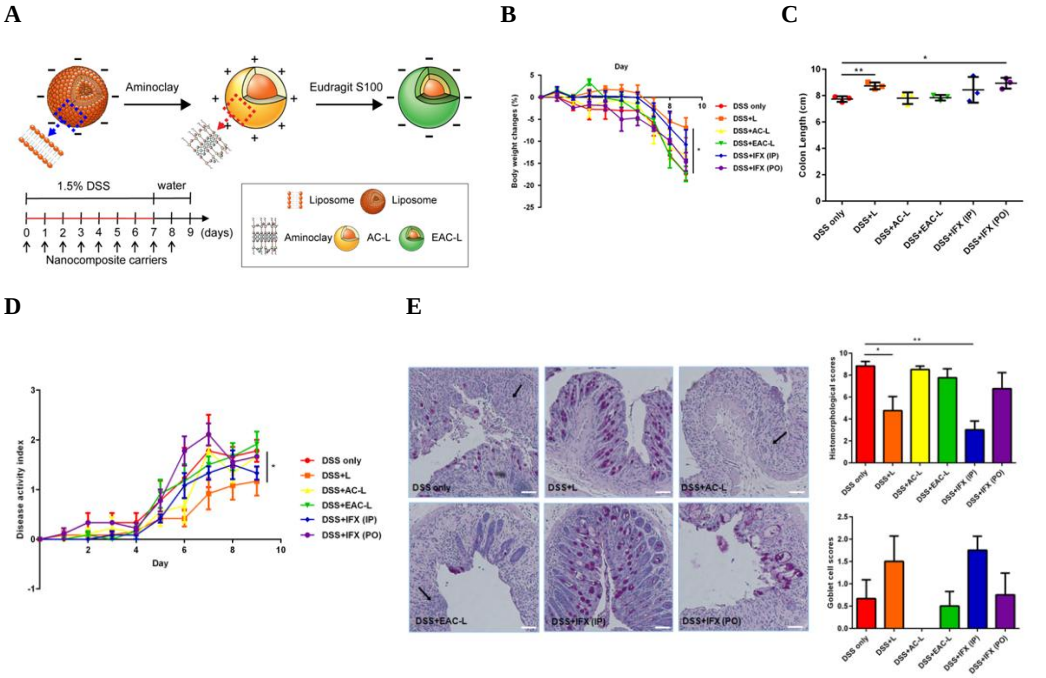

Figure 6. Therapeutic effect of nanocomposite carriers

Drug delivery system (DDS) ameliorates changes associated with inflamed mucosa in dextran sodium sulfate (DSS) colitis mice. C57/B6 mice were treated with vehicle control (n = 3), liposome (n = 4), aminoclay + liposome (n = 4), eudragitS100 +

aminoclay + liposome (n=4), intraperitoneal infliximab, (n = 4) and oral infliximab (n = 4). (A) Methods of administration of DSS-induced colitis and oral delivery carriers. (B) Body weight changes of each group in a DSS colitis mice model. (C) Colon length; values are represented as length (cm). Groups of DSS with liposome and DSS treated by oral infliximab showed significantly longer colons compared to DSS only group. (D) Histopathologic features of formulations of the DSS colitis mice model, via PAS staining. Arrows indicated inflammatory cells in the lamina propria. Scale bar: 20 μm. (E) Clinical activity scores in control group and treatment groups as measured using disease activity index (DAI), histomorphological score and goblet cell score. Data are expressed as means ± SD. * $p < 0.05$; **, $p < 0.01$; ***, $p < 0.001$; ****, $p < 0.0001$.

7. IFX-L, AC-IFX-L, and EAC-IFX-L deliver IFX to the targeted inflamed colon, resulting in therapeutic effect

To test the therapeutic effects of nanocomposite carriers loaded with IFX, mice were orally administered PBS, IFX-L, AC-IFX-L, EAC-IFX-L, or IFX (10 mg/kg, PO) daily from day 0 to day 8 (total 9 days). Colitis was induced by administering 1.5% DSS through drinking water for 7 days (Figure 7A). IFX-L, AC-IFX-L and EAC-IFX-L groups resulted in significantly less weight change, compared to the DSS-treated group (Figure 7B). All IFX delivery formulations with nanocomposite carriers had a significantly greater therapeutic effect in terms of colon length reduction and histopathological inflammatory cell infiltration, compared to the DSS-treated group (Figure 7C, E). There was no significant difference in colon shortening between the nanocomposite carriers themselves and the IFX encapsulated by nanocomposite carriers. There was a significantly higher improvement of DAI in the AC-IFX-L and EAC-IFX-L groups, compared to the DSS-treated group. (Figure 7D). Interestingly, EAC-IFX-L showed lower DAI value than EAC-L. All IFX delivery formulations with nanocomposite carriers showed significantly lower histomorphological scores than the DSS-treated group. The IFX-L group showed a higher goblet cell score than

the DSS-treated group (Figure 7E). AC-IFX-L group showed lower histomorphological scores and higher goblet cell scores than AC-L group. These results suggest that the conjugation of IFX to nanocomposite carriers preserves IFX function which successfully targets the colitis site.

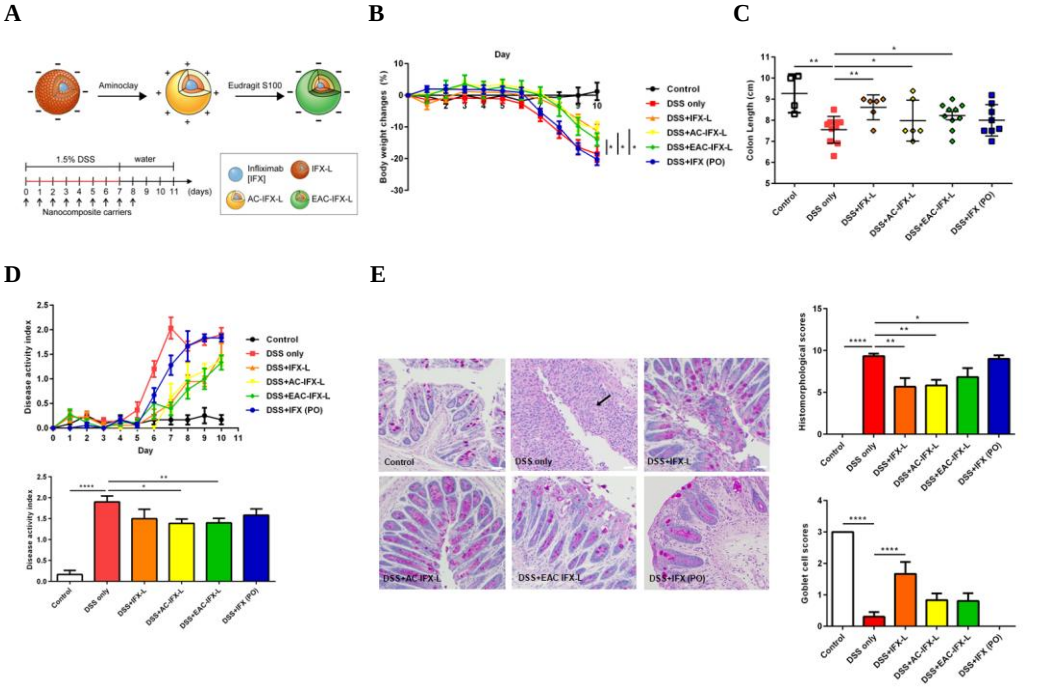

Figure 7. Therapeutic effects of drug delivery formulations showed in mice with dextran sulfate sodium (DSS)-induced colitis.

(A) The methods for DSS-induced colitis and oral delivery carriers with infliximab (IFX) administration, control (n = 4), DSS only (n = 10), L group (n = 6), AC-IFX-L (n = 6), EAC-IFX-L (n = 10), PO-IFX (n = 8) (B) body weight changes of each group in DSS-induced colitis mouse model. (C) colon length; values are represented as length (cm). (D) the clinical activity scores in the control group and treatment groups measured using the disease activity index (DAI). (E) histopathologic features of nanocomposite carriers and IFX delivery formulations on the DSS-induced colitis mouse model, via PAS staining. Arrows indicate inflammatory cells in the lamina propria. Scale bar: 20 μm. Histomorphological scores and Goblet cell scores. Data are

expressed as means ± SD. *, $p < 0.05$; **, $p < 0.01$; ***, $p < 0.001$; ****, $p < 0.0001$. Statistical significance was assessed using Student's t-test (D) and one-way ANOVA followed by Dunnett post-test.

8. Anti-inflammatory effect of nanocomposite carriers loaded with IFX

We used western blotting to investigate the effects of IFX delivery formulations on the protein expression of TNF-α and IL-1β. Induction of inflammation by DSS increased the expression of TNF-α and IL-1β, whereas protein expression in the EAC-IFX-L group was significantly decreased (Figure 8A). The expression of TNF-α in the AC-IFX-L group was also a significantly decreased, compared to the DSS only group.

As an indicator of therapeutic effect of the IFX delivery formulation against inflammation, TNF-α expression in serum extracted from mice was measured by ELISA. In the all IFX delivery formulations with nanocomposite carrier groups, the expression levels of TNF-α were significantly decreased compared to the DSS-treated control group (Figure 8B).

Inflammation-related factors (*Il1b*, *Tnfa*, *Il6*, *Il17* and *Inos*) were analyzed at the mRNA level in the DSS colitis colon after receiving IFX delivery formulation (Figure 8C). The IFX-L group exhibited significantly lower level of Tnfa and Il17 compared to the DSS-treated control group. Interestingly, the levels of Il1b and Il17, as well as Tnfa, were reduced in the AC-IFX-L and EAC-IFX-L groups. All drug delivery formulations showed no significant decrease in Inos and Il6 compared to the DSS-treated group. However, there was a larger fold change in mRNA levels of inflammation-related factors in the direct oral administration of IFX group without carriers than via drug delivery formulations, but this was no statistically significant difference (Figure 8D). Collectively, these results suggest that all drug delivery formulations with entrapped IFX successfully targeted *Tnfa* in the inflamed colon, and had an anti-inflammatory effect in a DSS-induced colitis model.

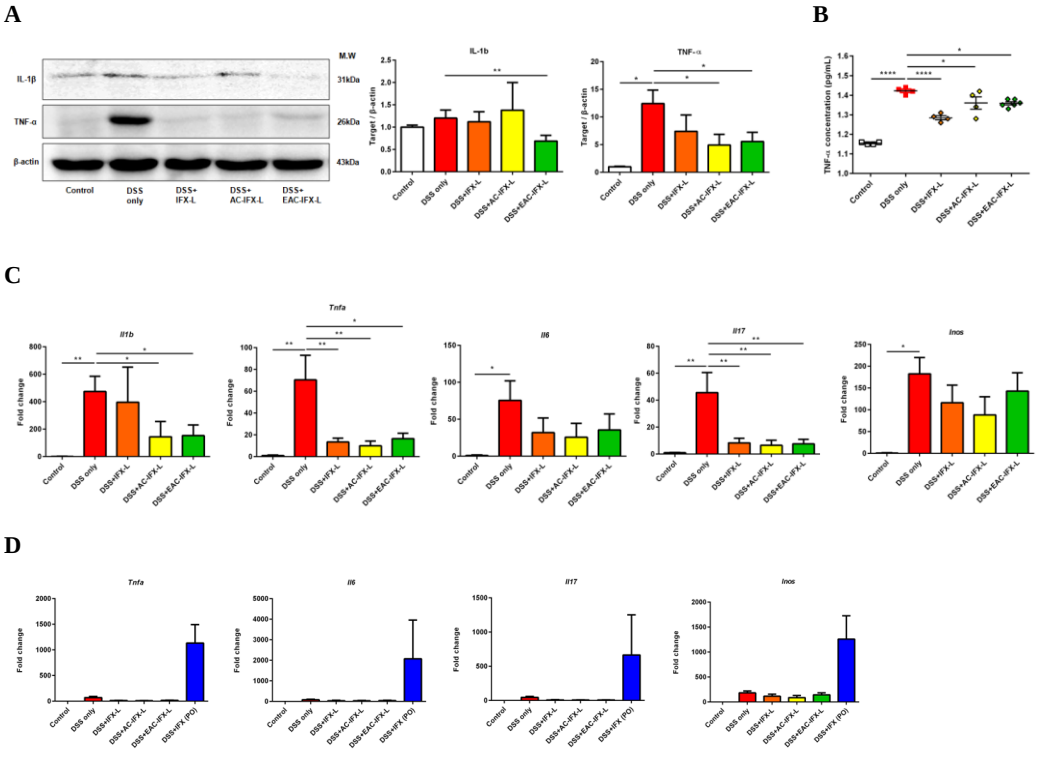

Figure 8. Anti-inflammatory effect of nanocomposite carriers loaded with IFX (A) Western blot analysis of protein expression of TNF-α and IL-1β in drug delivery formulations with IFX and their effects on the production and regulation of inflammation-related factors. Data are shown for colon. The ratios to beta-actin to standardize of cytokine protein expression in mice with DSS-induced colitis compared to control mice. (B) Expression of TNF-α by plasma of DSS colitis mice using ELISA. (C) Expression of inflammation-related factors in mRNA levels in the colon of DSS colitis mice treated by drug delivery IFX formulations. Gene expression was evaluated by quantitative RT-PCR. (D) Comparison of mRNA levels between oral administration of IFX drug delivery system and IFX itself. Gene expression were evaluated by quantitative RT-PCR and relative expression was reported as fold change compared to the control by normalizing transcription level to β-actin. Data are expressed as means ± SD. * $p < 0.05$; **, $p < 0.01$; ***, $p < 0.001$; ****, $p < 0.0001$. Statistical significance was assessed using Student's t-test (B-E) and one-way

ANOVA followed by Dunnett post-test.

IV. DISCUSSION

Colon-targeting oral drug delivery systems are quite an attractive therapeutic strategy for the treatment of diseases affecting the colon, such as IBD.[32,33] An ideal colon-specific delivery system maintains the maximum target-specific concentration of an entrapped drug, while minimizing systemic exposure by preventing premature drug release. The colon, a suitable delivery target site for proteinaceous drugs, has relatively limited proteolytic activity, compared to other parts of the gastrointestinal tract. The residence time of drugs in the colon is also relatively longer than that of other sites.[34,35] In this regard, the properties of surface coating materials and their interactions with liposomes are important determinants of the effects of liposome drug carriers targeting the colon. The efficiency of orally administered drugs delivered to the colon is improved by the polymer coating liposome formulation via pH-dependent release and mucosa-adhesive properties. In addition, phosphatidylcholine, a major component of the gastrointestinal membrane and liposome, reduces the inflammatory response and induces remission in UC patients.[36] Aminoclay is an excellent material for improving the bioavailability of poorly water-soluble drugs. The drug-clay complexes can regulate drug release properties by interacting with negatively charged drug molecules in water. Indeed, various delivery systems have been developed using Eudragit-coated liposome or aminoclay as efficient and versatile biocompatible carriers.[37,38] The charges of AC-L are made positive by the amino groups ($-NH_3$) of aminoclay and the charges of the anionic polymer nanoparticles of EAC-L are negative because of the carbonyl groups on the polymeric chain extremities. Overall, the results of the current study showed that nanocomposite carriers may be efficient oral delivery carriers in the treatment of IBD.

In this study, the degradation of nanocomposites entrapped with BSA was not significant in SGF and SIF (Figure 3), and the release rate of BSA in PBS and SIF was lower than that of free BSA. Normal pH ranges from 5.9 in the proximal colon to

6.1 in the distal colon. However, colon pH values in IBD patients vary significantly from pH 4.8 to 7.3.[39,40] Because bile salts and digestive enzymes (pancreatin) have a synergistic effect on the breakdown of liposome membranes in SIF, drug release rates usually increase in SIF, compared to SGF.[32,41] However, in this study, the difference in diameter change between SIF and SGF was minimal. Liposomes are less susceptible to pepsin alone and stable to pancreatin at neutral pH without bile salts.[42] The reason that results of the current study differ from previous studies may be because we did not mix bile salts with digestive enzymes that could break the integrity of liposome by solubilizing the membrane and forming temporary pores. However, the current study showed that the nanocomposite carriers are stable even at different pH levels, such as in the stomach or small intestine, and can reach the colon by maintaining stable drug concentrations for a long time. The stability of BSA was analyzed by circular dichroism spectroscopy which indicated that the α-helix structure of free BSA was broken after 1 h under SGF (pepsin +). However, the BSA in nanocomposite carriers retained a much better structure than free BSA, especially when EAC-L was included.

IBD patients are characterized by altered expression of tight junction proteins and loss of barrier integrity.[43,44] In addition, TNF-α, a pathological cytokine, increases epithelial permeability through changes in tight junction function and structure. In this study, we orally administered IFX targeting the colon using liposomes, aminoclay, and Eudragit S100-based nanocomposite carriers. In previous studies, *in vivo* image analysis by confocal microscopy confirmed the effective intracellular distribution of fluorescently labeled nanocomposite carriers in the colon.[24,45] The expression of each macrophage marker gene and the accumulation of liposomes showed a significant positive correlation, and liposomes enhanced the accumulation of drug candidates through macrophages in damaged colon tissue.[46] Our results suggest that liposome, aminoclay, and Eudragit S100 provide a colon-specific anti-inflammatory effect without adversely affecting systemic homeostasis. In addition, the fluorescence intensity of fluorescence-labeled liposomes is closely related to the expression levels of the macrophage marker. This indicates that the absorption mechanism of the

liposomes is related to the phagocytic property of macrophages.[46] Furthermore, a previous study of nanocomposite carriers using aminoclay and Eudragit in LPS-stimulated RAW 264.7 cells found no toxicity to macrophages.[23] The results of these publications, taken together with those of the current study, indicated that these nanocomposites may be good candidates as carriers for oral drug delivery (Figure 8). Since Eudragit degrades below pH 6.8, and the gastrointestinal tract in mice is shorter than that of humans, the therapeutic effects of EAC-L and EAC-IFX-L require further study. Importantly, our work provides additional insight into the development of orally administered nanocomponent carriers for the treatment of colitis. In addition, our method of coating IFX has already proven to be an effective approach in treating IBD and has the potential to be used in personalized medicine to provide a tailored oral delivery carrier because it reaches the colon and targets macrophages with unique biocompatibility and biodegradability.

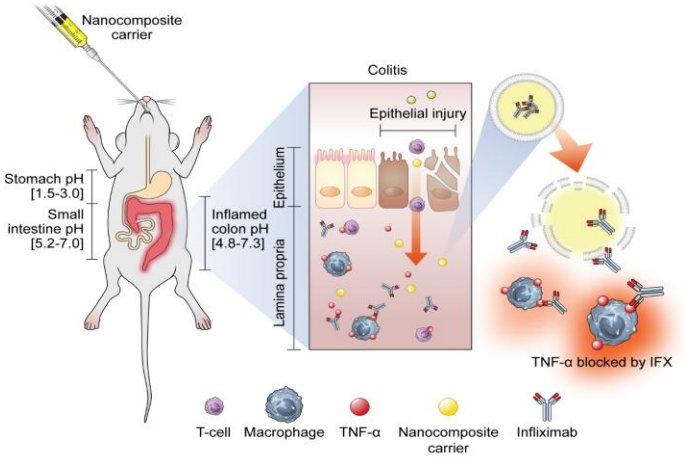

Figure 9. A putative model for the distribution and interaction with T cells and macrophages of nanocomposite carriers between normal colon and colitis condition.

Increased particle uptake due to epithelial leakage in colitis and infliximab [IFX] is active at the targeted colon: IFX reacts with macrophage and T cells in the colon to promote anti-inflammatory effects.

The increased secretion of TNF-α and IL1β in the colonic lamina propria has an important function in the development of IBD. UC patients have higher baseline levels of IL1β and TNF-α concentrations than those of CD patients.[48] IFX treatment increases the apoptosis of T lymphocytes in the intestinal mucosa.[49] The expression of Il17 is increased in the intestinal mucosa and serum of IBD patients.[50] The reduction of Il17 expression in the intestinal mucosa of IBD patients is closely associated with endoscopic response and mucosal healing after IFX treatment.[51] Our results indicate that drug delivery formulations significantly increased MFI values for lymphocytes in UC patients, while the mRNA expression of Tnfa, Il1b, and Il17 was significantly decreased.

Il1b and *Il17*, which are involved in the pathogenesis of IBD due to innate lymphoid cells and CD4+ Th17 cells, were significantly decreased in the EAC-IFX-L group.[52,53] Therefore, although our EAC-L data suggest that it is selectively taken by macrophages to improve DSS-induced mouse colitis, further studies on the molecular mechanisms regulating macrophage function are necessary. Our results indicate that carriers coated with liposomes alone and aminoclay-coated liposomes also contributed to anti-inflammatory responses. Further studies on the regulation of inflammatory cytokines by the carriers themselves are required to confirm their anti-inflammatory effects and those of liposomes.

V. CONCLUSION

All nanocomposite carriers loaded with IFX were prepared with narrow size distribution and high encapsulation efficiency. Theses nanocomposite carriers loaded with IFX provide a colon-specific anti-inflammatory effect without adversely affecting systemic homeostasis. Oral drug delivery by EAC-L may be a novel means of transporting large molecule drugs to the intestines in a non-cytotoxic way, to stimulate CD4+ T cells as well as macrophages. Furthermore, the unique propensity of EAC-L enhances anti-inflammatory responses of intestinal macrophages and provides attractive strategies for preventing or treating autoimmune diseases. All

nanocomposite carriers loaded with IFX had better colitis improvement than the control group. In addition, IFX treatment by AC-IFX-L and EAC-IFX-L-based nanocomposites not only showed a significant anti-inflammatory effect but also remarkably decreased TNF-α level in a DSS-induced mouse colitis model. This suggests that EAC-L can be a promising therapeutic approach for treating IBD.

REFERENCES

1. Perrier C, de Hertogh G, Cremer J, *et al.* Neutralization of membrane tnf, but not soluble tnf, is crucial for the treatment of experimental colitis. *Inflammatory bowel diseases* 2013;**19**:246-53.
2. Uhlig HH, Powrie F. Translating immunology into therapeutic concepts for inflammatory bowel disease. *Annual review of immunology* 2018;**36**:755-81.
3. Atreya R, Zimmer M, Bartsch B, *et al.* Antibodies against tumor necrosis factor (tnf) induce t-cell apoptosis in patients with inflammatory bowel diseases via tnf receptor 2 and intestinal cd14(+) macrophages. *Gastroenterology* 2011;**141**:2026-38.
4. Kamada N, Hisamatsu T, Okamoto S, *et al.* Unique cd14 intestinal macrophages contribute to the pathogenesis of crohn disease via il-23/ifn-gamma axis. *Journal of Clinical Investigation* 2008;**118**:2269-80.
5. Ordas I, Mould DR, Feagan BG, Sandborn WJ. Anti-tnf monoclonal antibodies in inflammatory bowel disease: Pharmacokinetics-based dosing paradigms. *Clinical pharmacology and therapeutics* 2012;**91**:635-46.
6. Levin AD, Wildenberg ME, van den Brink GR. Mechanism of action of anti-tnf therapy in inflammatory bowel disease. *Journal of Crohn's & Colitis* 2016;**10**:989-97.
7. Bryant RV, Burger DC, Delo J, *et al.* Beyond endoscopic mucosal healing in uc: Histological remission better predicts corticosteroid use and hospitalisation over 6 years of follow-up. *Gut* 2016;**65**:408-14.
8. Ooi CJ, Hilmi I, Banerjee R, *et al.* Best practices on immunomodulators and biologic agents for ulcerative colitis and crohn's disease in asia. *Intestinal research* 2019;**17**:285-310.
9. Nyboe Andersen N, Pasternak B, Basit S, *et al.* Association between tumor necrosis factor-alpha antagonists and risk of cancer in patients with inflammatory bowel disease. *The Journal of the American Medical Association* 2014;**311**:2406-13.
10. Colombel JF, Loftus EV, Jr., Tremaine WJ, *et al.* The safety profile of infliximab in patients with crohn's disease: The mayo clinic experience in 500 patients. *Gastroenterology* 2004;**126**:19-31.
11. Agarwal A, Kedia S, Jain S, *et al.* High risk of tuberculosis during infliximab therapy despite tuberculosis screening in inflammatory bowel disease patients

in india. *Intestinal research* 2018;**16**:588-98.
12. Kane SV, Chao J, Mulani PM. Adherence to infliximab maintenance therapy and health care utilization and costs by crohn's disease patients. *Advances in Therapy* 2009;**26**:936-46.
13. Bozzuto G, Molinari A. Liposomes as nanomedical devices. *International Journal of Nanomedicine* 2015;**10**:975-99.
14. Zhang R, Qian J, Li X, Yuan Y. Treatment of experimental autoimmune uveoretinitis with intravitreal injection of infliximab encapsulated in liposomes. *The British Journal of Ophthalmology* 2017;**101**:1731-8.
15. Kim JH, Hong SS, Lee M, *et al.* Krill oil-incorporated liposomes as an effective nanovehicle to ameliorate the inflammatory responses of dss-induced colitis. *International Journal of Nanomedicine* 2019;**14**:8305-20.
16. Yang L, Shao Y, Han HK. Improved ph-dependent drug release and oral exposure of telmisartan, a poorly soluble drug through the formation of drug-aminoclay complex. *International Journal of Pharmaceutics* 2014;**471**:258-63.
17. Kim SY, Lee SJ, Han HK, Lim SJ. Aminoclay as a highly effective cationic vehicle for enhancing adenovirus-mediated gene transfer through nanobiohybrid complex formation. *Acta Biomaterialia* 2017;**49**:521-30.
18. Coco R, Plapied L, Pourcelle V, *et al.* Drug delivery to inflamed colon by nanoparticles: Comparison of different strategies. *International Journal of Pharmaceutics* 2013;**440**:3-12.
19. Kshirsagar SJ, Bhalekar MR, Patel JN, Mohapatra SK, Shewale NS. Preparation and characterization of nanocapsules for colon-targeted drug delivery system. *Pharmaceutical Development and Technology* 2012;**17**:607-13.
20. Bautzova T, Rabiskova M, Beduneau A, Pellequer Y, Lamprecht A. Bioadhesive pellets increase local 5-aminosalicylic acid concentration in experimental colitis. *EuropeanJournal of Pharmaceutics and Biopharmaceutics* 2012;**81**:379-85.
21. Karn PR, Vanic Z, Pepic I, Skalko-Basnet N. Mucoadhesive liposomal delivery systems: The choice of coating material. *Drug Development and Industrial Pharmacy* 2011;**37**:482-8.
22. Hong SS, Kim SH, Lim SJ. Effects of triglycerides on the hydrophobic drug loading capacity of saturated phosphatidylcholine-based liposomes. *International Journal of Pharmaceutics* 2015;**483**:142-50.
23. Kim HY, Cheon JH, Lee SH, *et al.* Ternary nanocomposite carriers based on organic clay-lipid vesicles as an effective colon-targeted drug delivery system: Preparation and in vitro/in vivo characterization. *Journal of Nanobiotechnology* 2020;**18**:17.
24. Berlec A, Perse M, Ravnikar M, *et al.* Dextran sulphate sodium colitis in c57bl/6j mice is alleviated by lactococcus lactis and worsened by the neutralization of tumor necrosis factor alpha. *International*

Immunopharmacology 2017;**43**:219-26.

25. Lenzen H, Qian J, Manns MP, Seidler U, Jorns A. Restoration of mucosal integrity and epithelial transport function by concomitant anti-tnfalpha treatment in chronic dss-induced colitis. *Journal of Molecular Medicine (Berl)* 2018;**96**:831-43.
26. Seo DH, Che X, Kwak MS, *et al.* Interleukin-33 regulates intestinal inflammation by modulating macrophages in inflammatory bowel disease. *Scientific Reports* 2017;**7**:851.
27. Chassaing B, Aitken JD, Malleshappa M, Vijay-Kumar M. Dextran sulfate sodium (dss)-induced colitis in mice. *Current Protocols in Immunology* 2014;**104**:15.25.1-15.25.14.
28. Sharma M, Sharma V, Panda AK, Majumdar DK. Development of enteric submicron particle formulation of papain for oral delivery. *International Journal of Nanomedicine* 2011;**6**:2097-111.
29. Zenewicz LA, Antov A, Flavell RA. Cd4 t-cell differentiation and inflammatory bowel disease. *Trends in Molecular Medicine.* 2009;**15**:199-207.
30. Reinecker HC, Steffen M, Witthoeft T, *et al.* Enhanced secretion of tumour necrosis factor-alpha, il-6, and il-1 beta by isolated lamina propria mononuclear cells from patients with ulcerative colitis and crohn's disease. *Clinical and Experimental Immunology* 1993;**94**:174-81.
31. Lee SH, Kwon JE, Cho M-L. Immunological pathogenesis of inflammatory bowel disease. *Intestinal Research* 2018;**16**:26-42.
32. Yang M, Zhang F, Yang C, *et al.* Oral targeted delivery by nanoparticles enhances efficacy of an hsp90 inhibitor by reducing systemic exposure in murine models of colitis and colitis-associated cancer. *Journal of Crohn's and Colitis* 2020;**14**:130-41.
33. Zhang M, Xu C, Liu D, *et al.* Oral delivery of nanoparticles loaded with ginger active compound, 6-shogaol, attenuates ulcerative colitis and promotes wound healing in a murine model of ulcerative colitis. *Journal of Crohn's and Colitis* 2018;**12**:217-29.
34. Renukuntla J, Vadlapudi AD, Patel A, Boddu SH, Mitra AK. Approaches for enhancing oral bioavailability of peptides and proteins. *International Journal of Pharmaceutics* 2013;**447**:75-93.
35. McConnell EL, Liu F, Basit AW. Colonic treatments and targets: Issues and opportunities. *J Drug Target* 2009;**17**:335-63.
36. Karner M, Kocjan A, Stein J, *et al.* First multicenter study of modified release phosphatidylcholine "lt-02" in ulcerative colitis: A randomized, placebo-controlled trial in mesalazine-refractory courses. *American Journal of Gastroenterology* 2014;**109**:1041-51.
37. Barea MJ, Jenkins MJ, Lee YS, Johnson P, Bridson RH. Encapsulation of liposomes within ph responsive microspheres for oral colonic drug delivery. *International Journal of Biomaterials* 2012;**2012**:458712-.
38. Kim SY, Kwon WA, Shin SP, *et al.* Electrostatic interaction of tumor-

targeting adenoviruses with aminoclay acquires enhanced infectivity to tumor cells inside the bladder and has better cytotoxic activity. *Drug Delivery* 2018;**25**:49-58.

39. Nugent SG, Kumar D, Rampton DS, Evans DF. Intestinal luminal ph in inflammatory bowel disease: Possible determinants and implications for therapy with aminosalicylates and other drugs. *Gut* 2001;**48**:571-7.
40. Press AG, Hauptmann IA, Hauptmann L, *et al.* Gastrointestinal ph profiles in patients with inflammatory bowel disease. *Alimentary Pharmacology & Therapeutics* 1998;**12**:673-8.
41. Nguyen TX, Huang L, Liu L, *et al.* Chitosan-coated nano-liposomes for the oral delivery of berberine hydrochloride. *Journal of Materials Chemistry B* 2014;**2**:7149-59.
42. Hu S, Niu M, Hu F, *et al.* Integrity and stability of oral liposomes containing bile salts studied in simulated and ex vivo gastrointestinal media. *International Journal of Pharmaceutics* 2013;**441**:693-700.
43. Capaldo CT, Nusrat A. Claudin switching: Physiological plasticity of the tight junction. *Semin Cell and Developmental Biology* 2015;**42**:22-9.
44. Cornick S, Tawiah A, Chadee K. Roles and regulation of the mucus barrier in the gut. *Tissue Barriers* 2015;**3**:e982426.
45. Maisel K, Ensign L, Reddy M, Cone R, Hanes J. Effect of surface chemistry on nanoparticle interaction with gastrointestinal mucus and distribution in the gastrointestinal tract following oral and rectal administration in the mouse. *Journal of Controlled Release* 2015;**197**:48-57.
46. Yamasaki M, Muraki Y, Nishimoto Y, Murakawa Y, Matsuo T. Fluorescence-labeled liposome accumulation in injured colon of a mouse model of t-cell transfer-mediated inflammatory bowel disease. *Biochemical and Biophysical Research Communications* 2017;**494**:188-93.
47. Harris MS, Hartman D, Lemos BR, *et al.* Avx-470, an orally delivered anti-tumour necrosis factor antibody for treatment of active ulcerative colitis: Results of a first-in-human trial. *Journal of Crohn's and Colitis* 2016;**10**:631-40.
48. Lacruz-Guzman D, Torres-Moreno D, Pedrero F, *et al.* Influence of polymorphisms and tnf and il1beta serum concentration on the infliximab response in crohn's disease and ulcerative colitis. *European Journal of Clinical Pharmacology* 2013;**69**:431-8.
49. ten Hove T, van Montfrans C, Peppelenbosch MP, van Deventer SJ. Infliximab treatment induces apoptosis of lamina propria t lymphocytes in crohn's disease. *Gut* 2002;**50**:206-11.
50. Fujino S, Andoh A, Bamba S, *et al.* Increased expression of interleukin 17 in inflammatory bowel disease. *Gut* 2003;**52**:65-70.
51. Caprioli F, Bose F, Rossi RL, *et al.* Reduction of cd68+ macrophages and decreased il-17 expression in intestinal mucosa of patients with inflammatory bowel disease strongly correlate with endoscopic response and mucosal

healing following infliximab therapy. *Inflammatory Bowel Diseases* 2013;**19**:729-39.

52. Coccia M, Harrison OJ, Schiering C, *et al.* Il-1beta mediates chronic intestinal inflammation by promoting the accumulation of il-17a secreting innate lymphoid cells and cd4(+) th17 cells. *Journal of Experimental Medicine* 2012;**209**:1595-609.
53. Gálvez J. Role of th17 cells in the pathogenesis of human ibd. *International Scholarly Research Notices Inflammation* 2014;**2014**:928461-.

ABSTRACT (IN KOREAN)

대장염 마우스 모델에서 nanocomposites 을 기반으로 한 infliximab 과 경구 약물 전달 시스템

<지도교수 천재희>

연세대학교 대학원 의학과

김정민

종양괴사인자-알파를 차단하는 키메라 단클론항체인 infliximab (IFX)은 염증성 장질환 환자에서 임상적 호전 및 점막 치유를 유도한다. 그러나 이 약제는 전신 투여와 관련하여 원치 않는 전신 부작용을 일으킬 수 있다. 항체 치료제의 경구 전달은 통상적인 투여 경로와 비교하여 염증성 장질환에 대한 효과적인 치료 전략으로서 주목된다. 우리는 세 가지 물질을 이용한 나노 복합체 담체를 사용하여 infliximab의 경구 투여를 통해 대장 특이 약물 전달 시스템을 개발하고자 하였다.

liposome, Aminoclay로 코팅한 리포좀 (AC-L), Eudragit® S100과 Aminoclay로 코팅한 liposome (EAC-L) 또는 IFX (IFX-L, AC-IFX-L 및 EAC-IFX-L)를 포함하는 나노 복합체 담체를 dextran sulfate sodium으로 대장염을 유발시킨 마우스에 경구 투여하고 치료 효과와 염증 완화 효과 여부를 확인하였다. 염증성 장질환

환자의 말초 혈액 단핵 세포에서 림프구 및 단핵구에 대한 나노 복합체 담체의 효과를 확인하였고, 마우스 실험과 시험관 실험을 통해서 나노 복합체 자체의 치료 효과 및 IFX를 함유한 나노 복합체의 치료 효과를 평가하였다.

3 가지의 나노 복합체 담체들은 모두 높은 캡슐화 효율, 좁은 크기 분포 및 최소의 시스템 노출을 가졌다. 그리고, 염증성 장질환 환자의 말초혈액 단핵 세포에서 림프구에 비해 나노 복합체 담체들과 단핵구들 사이의 높은 상호 작용을 확인했다. 마우스의 염증성 대장염에 표적으로 경구 투여된 나노 복합체 담체들은 전신 노출이 대조군보다 적었고, 경구 투여한 리포좀은 대장염의 증상을 완화시켰다. AC-IFX-L 및 EAC-IFX-L은 유의한 치료 효과를 보였고 염증성 사이토카인 발현을 완화시켰다 (Tnfa, Il1b 및 Il17).

경구 투여 된 항체 전달 시스템은 전신 노출을 감소시키면서 염증성 장 질환에서 개선된 효능을 나타냈으며, 이러한 경구 약물 전달 시스템은 추후 염증성 장 질환의 치료를 위한 유망한 치료 방법으로 제시할 수 있을 것이다.

핵심되는 말: 염증성 장질환, 리포좀, infliximab, 나노 복합체 담체, 경구 전달 시스템

s